LEVEL II

(11)

AFGL-TR-80-0177

(9) ENVIRONMENTAL RESEARCH PAPERS, NO. 703

AD A092593

(6)

Comparison of the EMI Long Sea Path Transmittance Measurements With LOWTRAN 5 Calculations.

WILLIAM O. GALLERY

(10)

(14) AFGL-TR-80-0177, AFGL-ERP-703

(11) 28 May 1980

(12) 40

(16) 7670

(17) 09

Approved for public release; distribution unlimited.

OPTICAL PHYSICS DIVISION PROJECT 7670

AIR FORCE GEOPHYSICS LABORATORY

HANSCOM AFB, MASSACHUSETTS 01731

AIR FORCE SYSTEMS COMMAND, USAF

DISCLAIMER NOTICE

THIS DOCUMENT IS BEST QUALITY PRACTICABLE. THE COPY FURNISHED TO DTIC CONTAINED A SIGNIFICANT NUMBER OF PAGES WHICH DO NOT REPRODUCE LEGIBLY.

This report has been reviewed by the ESD Information Office (OI) and is releasable to the National Technical Information Service (NTIS).

This technical report has been reviewed and is approved for publication.

FOR THE COMMANDER

John Howard

Chief Scientist

Qualified requestors may obtain additional copies from the Defense Technical Information Center. All others should apply to the National Technical Information Service.

Unclassified

SECURITY CLASSIFICATION OF THIS PAGE (When Data Entered)

REPORT DOCUMENTATION PAGE		READ INSTRUCTIONS BEFORE COMPLETING FORM
1. REPORT NUMBER AFGL-TR-80-0177	2. GOVT ACCESSION NO. AD-A092 593	3. RECIPIENT'S CATALOG NUMBER
4. TITLE (and Subtitle) COMPARISON OF THE EMI LONG SEA PATH TRANSMITTANCE MEASUREMENTS WITH LOWTRAN 5 CALCULATIONS		5. TYPE OF REPORT & PERIOD COVERED Scientific. Interim.
		6. PERFORMING ORG. REPORT NUMBER ERP No. 703
7. AUTHOR(s) William O. Gallery		8. CONTRACT OR GRANT NUMBER(s)
9. PERFORMING ORGANIZATION NAME AND ADDRESS Air Force Geophysics Laboratory (OPI) Hanscom AFB Massachusetts 01731		10. PROGRAM ELEMENT, PROJECT, TASK AREA & WORK UNIT NUMBERS 62101F 7670 0906
11. CONTROLLING OFFICE NAME AND ADDRESS Air Force Geophysics Laboratory (OPI) Hanscom AFB Massachusetts 01731		12. REPORT DATE 28 May 1980
		13. NUMBER OF PAGES 40
14. MONITORING AGENCY NAME & ADDRESS(if different from Controlling Office)		15. SECURITY CLASS. (of this report) Unclassified
		15a. DECLASSIFICATION/DOWNGRADING SCHEDULE

16. DISTRIBUTION STATEMENT (of this Report)

Approved for public release; distribution unlimited.

17. DISTRIBUTION STATEMENT (of the abstract entered in Block 20, if different from Report)

18. SUPPLEMENTARY NOTES

19. KEY WORDS (Continue on reverse side if necessary and identify by block number)

Aerosols
Water vapor continuum
Atmospheric transmission model
Infrared absorption measurements
Maritime aerosols

20. ABSTRACT (Continue on reverse side if necessary and identify by block number)

A series of broadband visible and infrared transmittance measurements made by EMI Ltd. over a 20 km sea path are compared to transmittances calculated by LOWTRAN 5. The purpose of the comparison is primarily to test the validity of the Maritime aerosol model in LOWTRAN under realistic conditions, and incidentally to test the molecular extinction in several window regions. The results of this comparison are the following: (a) the Maritime aerosol model provides a good description of aerosol extinction for conditions

Micron

of a moderate wind blowing over the open ocean; (b) the calculated molecular extinction in the 8 to 12 μ region is accurate to within 7 percent in the log of the transmittance, although there is an indication the water vapor continuum absorption coefficient may be slightly too large; (c) the calculated molecular extinction in the 4.5 to 5.0 μ region is seriously underpredicted due to the lack of a water vapor continuum in this region.

Preface

The author wishes to thank Frank Kneizys and Eric Shettle for many helpful discussions in performing this work. The assistance of EMI Electronics Ltd. in making available their transmittance data is gratefully acknowledged. EMI Electronics Ltd. have requested us to point out that their data was obtained while working under contract to the Procurement Executive, Ministry of Defense, United Kingdom whose assistance in making the data available is also gratefully acknowledged.

Contents

Illustrations

Illustrations

Tables

Comparison of the EMI Long Sea Path Transmittance Measurements With LOWTRAN 5 Calculations

1. INTRODUCTION

During January and February, and again during August and September 1970, EMI Electronics Ltd. made a series of transmittance measurements along a long path over the ocean. Measurements were made for six broadband filters covering the visible and infrared windows from 0.5 μ to 12 μ. This report describes the comparison of these measurements with transmittances calculated using LOWTRAN 5. The purpose of the comparison is primarily to test the validity of the Maritime aerosol model in LOWTRAN 5 under real atmospheric conditions. In addition, these measurements include cases in which aerosol extinction is relatively small in the 4.5 to 5.0 and 8 to 12 μ window regions compared to the molecular absorption. These cases permit the testing of the LOWTRAN model for molecular absorption alone in these window regions.

(Received for publication 28 May 1980)

2. DESCRIPTION OF THE MEASUREMENTS

2.1 Apparatus

The EMI measurements[1] are documented and will be described here only briefly. The transmittance measurements were made along a 20 km path across Mounts Bay, Cornwall, at the southwestern coast of England. Figure 1a shows the relation of Mounts Bay to the large scale geography of the area, and Figure 1b shows a map of Mounts Bay itself. This site was chosen because it was the available site most representative of open sea conditions.

The source for the transmittance measurements was a carbon arc blackbody operating at 3800 K while the receiver was a Golay detector mounted at the focus of a 76 cm diameter mirror. Various filters could be placed in front of the detector. The filter response functions of the filters are shown in Figure 2a. Filters 1 to 5, corresponding to 0.57 - 0.97 μ, 1.55 - 1.75 μ, 2.05 - 2.3 μ, 3.4 - 4.2 μ, and 7.9 - 11.3 μ were used in both the winter (January - February) and in the summer (August - September) measurement series. For the summer series only, filter #6, covering 4.2 - 5.1 μ, was added.

The locations of the filters can be compared to the locations of the atmospheric windows shown in Figure 2b. This figure shows a plot of the atmospheric transmittance calculated by LOWTRAN from 0.2 to 14 μ for a 20 km horizontal path at sea level, with a pressure of 1 atm, temperature of 10° C, relative humidity of 70 percent, and a meteorological range of 50 km using the Maritime aerosol model; these conditions are typical of the conditions encountered during the EMI measurement series. It can be seen that the EMI filters were selected to cover the major atmospheric windows.

In addition to the transmittance, other physical parameters were measured including:

1. air temperature
2. relative humidity - from a wet and dry bulb thermometer
3. wind speed - estimated according to the Beaufort Scale
4. wind direction
5. sea state - estimated according to the Beaufort Scale
6. visibility - estimated by an observer viewing six landmarks around Mounts Bay
7. tide height

Indicators of the presence of rain or beam-bending effects were also recorded.

---

1. Arnold, D. H., Lake, D. B., and Sanders, R. Comparative Measurements of Infrared Transmission Over a Long Sea Path, E.M.I. Reports DMP 3736 (1970) and DMP 3858 (1971).

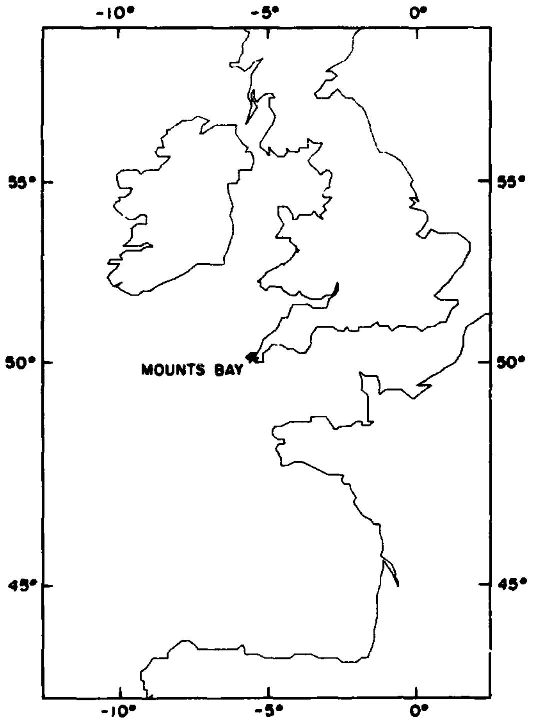

Figure 1a. Map showing the location of Mounts Bay, England relative to the large scale geography of the area

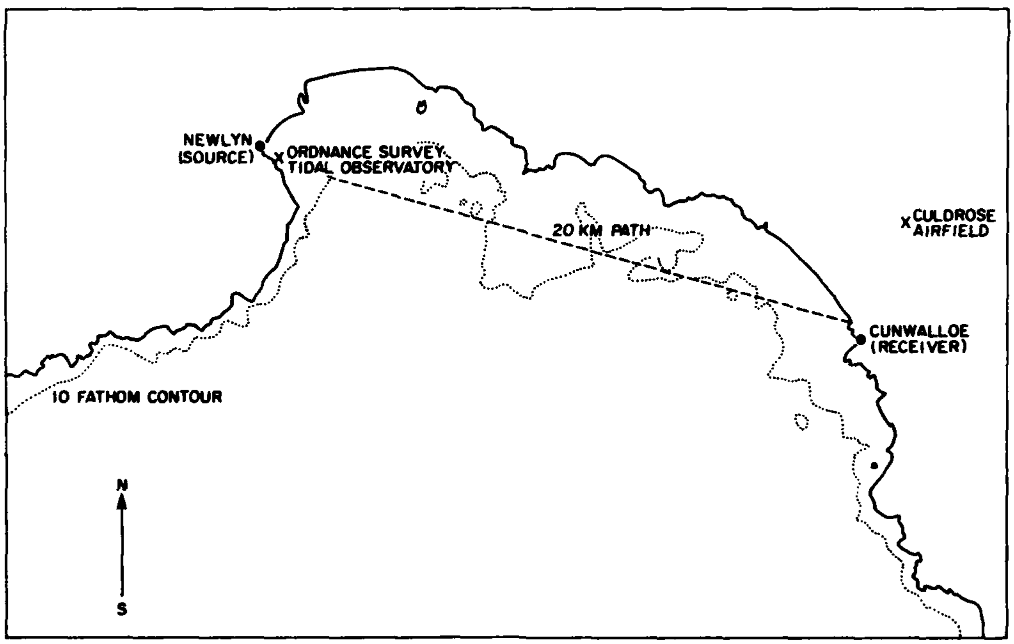

Figure 1b. Map of Mounts Bay, showing the location of the source and the receiver (from (1)).

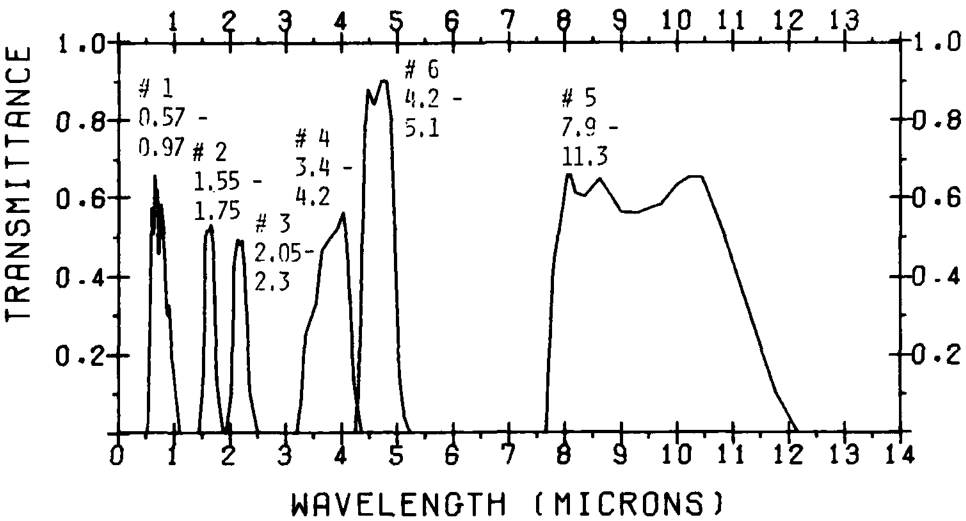

Figure 2a. Filter response functions for the 6 filters: #1 0.57 - 0.97 u; #2 1.55 - 1.75 µ; #3 2.05 - 2.3 u; #4 3.4 - 4.2 u; #5 7.9 - 11.3 u; #6 4.2 - 5.1 µ (summer series only)

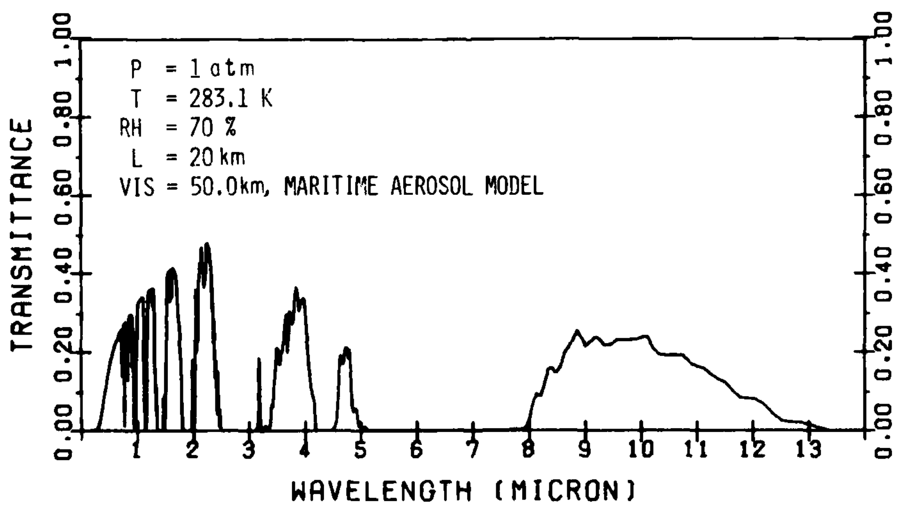

Figure 2b. LOWTRAN calculation from 0.2 to 14 u, for conditions typical of the EMI measurement series

2.2 Data Recording

Each block of data consists of the measurement of the physical parameters listed above followed by the measurement of the transmittance for the 5 or 6 filters. (Transmittance measurements were also made for a 0.63 μ He-Ne laser and a 10.6 μ CO_2 laser but these data will not be analyzed here.) The physical parameters were recorded on the data tape as integers from 1 to 39, resulting in the temperature being given to the nearest degree and the relative humidity to ± 1 percent. (The accuracy of the relative humidity is, however, certainly less than this.) The visibility was recorded to the nearest 1 km up to 37 km, or as simply 38 km or greater. The transmittances were recorded as the digital voltmeter readings of the amplified detector output. Translating the voltage readings to absolute transmittance is described in the next section.

Possible deficiencies in the data should be noted. The temperature and relative humidity were recorded at the receiver site on the beach, while most of the path was over open water. The recorded values, therefore, may not be representative of the values over the actual path. Also, the visibility measurements were made by observing landmarks inland of the bay and may not be representative of conditions along the path which may include wind-raised sea spray or low-lying fog or haze. The cutoff at 38 km is also a problem; a visibility of 38 km over a path of 20 km translates to a transmission in the visible of 13 percent. Since the meteorological range* is a required input to the aerosol extinction portion of LOWTRAN, using the observer-estimated visibility leaves a large uncertainty in the aerosol extinction at the shorter wavelengths for visibilities greater than 38 km. Finally, the observer-estimated measurement is largely subjective and prone to significant errors.

There are a total of 379 blocks of data with block numbers running from 127 to 506. Within a block, however, certain data, including both physical parameters or transmittances, may be missing, and in certain cases the measurements were affected by obscuration due to rain or by beam-bending effects. Blocks for which any of the temperature, relative humidity, or the transmittance for filter 1 were

---

* Visibility is defined as the greatest distance at which it is just possible to see and identify with the unaided eye: (a) in the daytime, a dark object against the horizon sky; and (b) at night, a known, moderately intense light source. Meteorological range V is defined as the distance over which the transmittance at 0.55 μ equals the threshold value of 0.02 and is given by Koschmieder's formula:

$$V = -\ln(0.02)/\sigma = 3.912/\sigma$$

where σ is the extinction coefficient at 0.55 μ.

Visibility and meteorological range are connected by the fact that the minimum detectable contrast for a dark object against a horizon sky has been found experimentally to be 0.02.

missing were rejected, since these three values are all needed as inputs to the LOWTRAN calculations. Blocks affected by obscuration due to rain or by beam-bending effects were also rejected since these effects are not adequately characterized in the measurements. In other cases, measurements for specific filters in particular blocks were rejected since they were obviously too low by an order of magnitude. After these deletions, 281 blocks of usable data remained.

2.3 Calibration

Calibration of the transmittance measurements was done by EMI in two steps: first, the response of each filter relative to the 7·9 to 11·3 μ filter was measured with the receiver located 52 m from the source. The atmospheric attenuation for this path in the spectral regions of interest was assumed to be negligible except for the 4·2 to 5·1 μ filter where correction was made for the very strong CO_2 absorption around 4·3 μ.

Next, for measurements along the 20 km path, let T_{ij} be the transmittance and S_{ij} the product of the detector output, the amplifier gain factor and the relative filter response factor for filter j and block i:

$$T_{ij} = C\, S_{ij} \quad . \tag{1}$$

The absolute calibration factor C was determined by estimating the transmittance T_o for filter 5 (7·9 to 11·3 μ) for the data block with the highest transmittance for filter 5 (block 257):

$$C = \frac{T_o}{S_{257,5}} \quad . \tag{2}$$

T_o was calculated using the data in Refs 2 and 3 to be 0.368.[2, 3]

The transmittance data as written on the data tape was actually presented as an "effective atmosphere extinction coefficient" σ_{ij} given as:

$$\sigma_{ij} = (\ln T_{ij})/L = [\ln C + \ln S_{ij}]/L \tag{3}$$

---

2. Altshuler, T. L., Infrared Transmission and Background Radiation by Clear Atmospheres, General Electric Co. Missile and Space Vehicle Department, Valley Forge, PA, Report No. 61SD19 (Dec 1961) (Available from NTIS - Accession Number AD 401923).

3. Hudsen, K. D. (1969) Infrared Systems Engineering, Ch 4, John Wiley and Sons, New York.

where L = 20 km is the path length. Note that this "extinction coefficient" is merely the log of the transmittance and is not comparable to a band model extinction coefficient. For the calibration case, the estimated value of T_o gave:

$$\sigma_o = -(\ln T_o)/L = 0.05\ \mathrm{km}^{-1} \quad . \tag{4}$$

The calibration is based on old data and may contain a substantial error. The error due to calibration in any value of σ_{ij}, however, will equal the error in σ_o; that is, the magnitude of the error is independent of both the filter and the case. The question of calibration will be dealt with further in the comparison of the measurements with the LOWTRAN calculations.

3. LOWTRAN CALCULATIONS

3.1 General

Transmittances corresponding to the measured values were calculated using a modified version of "LOWTRAN 5."[4] This version contained four relative-humidity-dependent aerosol models[5] - Rural, Maritime, Urban, Tropospheric - and contained a subroutine to convolve the transmittance with a user-defined filter function.

The EMI filter functions are shown in Figure 2a. The filter functions $F(\tilde{\nu})$ were digitized and then interpolated to the LOWTRAN wavenumbers. The average transmission over a filter is then calculated by

$$\overline{T} = \int T(\tilde{\nu}) B(\theta, \tilde{\nu}) F(\tilde{\nu}) d\nu \Big/ \int B(\theta, \tilde{\nu}) F(\tilde{\nu}) d\tilde{\nu} \tag{5}$$

where $T(\tilde{\nu})$ is the transmittance and $B(\theta, \tilde{\nu})$ is the blackbody function at temperature of the source θ and at wavenumber $\tilde{\nu}$.

The other inputs to the LOWTRAN calculations are air temperature, relative humidity, air pressure, path length, aerosol model, and meteorological range. The air pressure was taken to be 1013.25 mb and the path length 20 km. The temperature and relative humidity were the appropriate values for each block of data.

---

4. Kneizys, F. X., Shettle, E. P., Gallery, W. O., Chetwynd, J. H., Jr., Abreu, L. W., Selby, J. E. A., Fenn, R. W., and McClatchey, R. A. (1980) Atmospheric Transmittance/Radiance: Computer Code LOWTRAN 5, AFGL-TR-80-0067.

5. Shettle, E. P. and Fenn, R. W. (1979) Models for the Aerosols of the Lower Atmosphere and the Effects of Humidity Variations on Their Optical Properties, AFGL-TR-79-0214.

3.2 Aerosol Model and Meteorological Range

It was not clear initially what the appropriate values were to use for the aerosol model and for the meteorological range. Each of the various aerosol models in LOWTRAN were derived based on a specific particle size distribution found to be representative of that particular air mass type. From the particle size distribution, the wavelength dependence of the aerosol extinction coefficient relative to 0.55 u is calculated from Mie scattering theory. It is this wavelength dependence, b(λ), of the aerosol extinction coefficient which characterizes each aerosol model in LOWTRAN; Figure 3 (from 5) shows this dependence for the various models. Note that the Maritime model drops off the least with increasing wavelength; this is due to the relatively large number of large sea-spray-produced particles contained in this model.

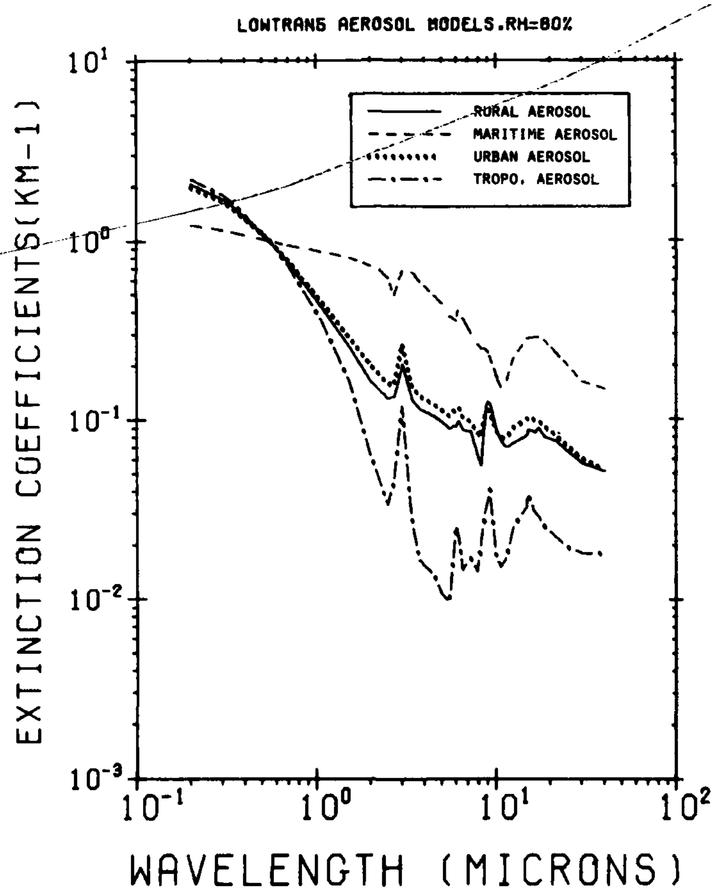

Figure 3. Normalized extinction coefficient (equals 1.0 at 0.55 u) vs wavelength for the four aerosol models in LOWTRAN 5

The geography of the experimental site would seem to indicate the use of the Maritime aerosol model in the LOWTRAN calculations, especially when the wind is onshore. The actual conditions occurring on a specific day, however, may not be described well by this model and may be described better by another model. It is also possible that none of the available models provides a good representation of the prevailing conditions. The suitability of some of the different models under different conditions will be tested here.

The value to use for the meteorological range V also presented a problem. As mentioned before, the observer-estimated value of the visibility is inaccurate and limited to visibilities less than 39 km. Now, by definition, the meteorological range V is given by Koschmieder's Law:

$$V = \frac{3.912}{\sigma_{.55}} \tag{6}$$

where $3.912 = -\ln(0 \cdot 02)$ and $\sigma_{.55}$ is the extinction coefficient at $0.55\,\mu$. While $\sigma_{.55}$ was not measured directly in this experiment, filter 1 did measure the extinction in the range from 0.57 to $0.97\,\mu$. The fact that between 0.55 and $1.0\,\mu$ the molecular extinction is relatively small and the wavelength dependence of the aerosol extinction coefficient is weak, at least for the Maritime model, suggests that V can be estimated from the extinction in filter 1 in the following manner.

The aerosol extinction at the wavelength λ for a given aerosol model is given by:

$$\sigma(\lambda) = b(\lambda)\,\sigma_{.55} \tag{7}$$

where $b(\lambda)$ is the relative extinction coefficient shown in Figure 3 for the various models. (The relative humidity dependence of $b(\lambda)$ will be neglected here.) From Eq. (6) and (7), one can write formally

$$V = 3.912\,\frac{b(\lambda)}{\sigma(\lambda)} \,. \tag{8}$$

Eq. (8) suggests that V can be determined from the equation

$$V = 3.912\,\frac{\beta}{\sigma_1{}^*} \tag{9}$$

where β is a constant and $\sigma_1{}^*$ is the measured effective extinction in filter 1. The constant β is chosen so that when V from Eq. (9) is input to LOWTRAN, LOWTRAN then calculates the same value of the mean effective extinction coefficient as was

measured. A single value of β is used for each aerosol model and it is determined empirically; for the Maritime model, β was found to be 0.924.

Figure 4 shows a plot of the calculated vs the measured effective extinction coefficients for filter 1 for all the 281 usable cases in the EMI data set. Note that although a single value of β is used for all the cases, in all cases the calculated value of the effective extinction coefficient is very nearly equal to the measured value. The fact that the agreement is excellent, however, is not physically significant and does not by itself justify this method of determining V. The justification for Eq. (9) lies in the agreement between the calculated and the measured data for the other filters, which will be demonstrated later.

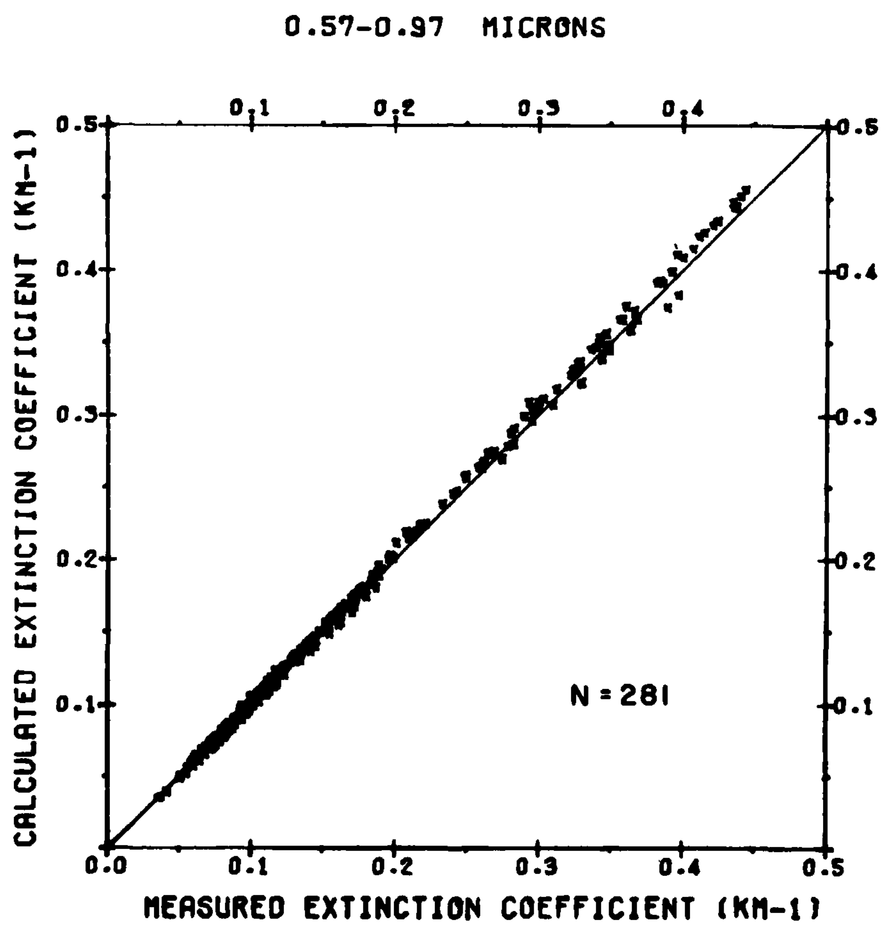

Figure 4. Calculated vs measured "effective extinction coefficients" for filter 1 for all the 281 usable cases in the EMI data set

4. COMPARISON OF MEASURED AND CALCULATED EXTINCTION COEFFICIENTS

4.1 Method of Analysis

Since the measured and calculated transmittances span four orders of magnitude, it is necessary to present the data in the form of the "effective extinction coefficients"; that is, $-(\ln \bar{T})/L$. In Figure 5 following, the calculated "effective extinction coefficient" is plotted vs the measured. The solid line in each figure is drawn at 45°. Also shown on each figure is the number of data points N and the correlation coefficient r between the calculated and the measured values. The dashed line, if shown, represents a simple least squares fit of the calculated to the measured data; the slope of the regression line is given by b, the y intercept by y_o, and the standard deviation about the regression line by s.

If x_i and y_i represent the measured and the calculated values, respectively, then these quantities are given by

$$r = \Sigma(x_i-\bar{x})(y_i-\bar{y})/[\Sigma(x_i-\bar{x})^2\Sigma(y_i-\bar{y})^2]^{1/2}$$

$$b = \Sigma(x_i-\bar{x})(y_i-\bar{y})/\Sigma(x_i-\bar{x})^2$$

$$y_o = \bar{y}-b\bar{x}$$

$$s^2 = \Sigma(y_i-(y_o+bx_i))^2/(N-2) \quad . \tag{10}$$

In the case of regression through the origin

$$y_o = o$$

$$b = \Sigma x_i y_i/\Sigma x_i^2 \quad . \tag{11}$$

Note, however, that simple least squares theory is not strictly applicable in this case, since both the measured and the calculated data contain errors. Furthermore, it is not clear what the appropriate weights are to use in the least squares; if the uncertainty in the transmittance is proportional to the transmittances, then in the least squares fit of the "effective extinction coefficients" (i.e., $\ln \bar{T}$) the data should have equal weights. If, however, the uncertainty in the transmittance is constant in transmittance, then the "effective extinction coefficients" should be weighted by $\bar{T}^2$. For the calculated transmittances, it appears reasonable

that the uncertainty is at least approximately proportional to the transmittances, since the uncertainty is primarily in the absorption coefficients and in the absorber amounts. The experimental error for the measured transmittances is not specified in the EMI reports, but since the measured transmittances span four orders of magnitude, it is unlikely that the error in transmittance is constant over that whole range. Of course, there must be a minimum absolute transmittance error set by the systems noise, but it is not clear what this level is, or whether it is approached by the measurements. As will be seen later, the agreement between the measured and the calculated extinctions for the highest values of extinction indicates that the uncertainty for large values of extinction is no greater than for small values.

With these considerations in mind, it will be assumed here that the uncertainty in the transmittance is proportional to the transmittance so that the extinction coefficients should be weighted equally in the least squares fit. The regression line derived from the least squares fit should give a reasonable fit to the data. It should be kept in mind, however, that simple least squares theory is not strictly applicable here, and that the weighting of the data is not necessarily correct. For these reasons, conclusions based on the slope and intercept of the regression line should be made cautiously.

Using the meteorological range given by Eq. (9) and the Maritime aerosol model, LOWTRAN was used to calculate the "effective extinction coefficients" for the remaining five filters for all the usable cases in the EMI data set; these data are shown in Figures 5a to e.

These figures show a strong correlation between the calculated and the measured data; the correlation coefficients range from 0.8 to 0.9. There is considerable scatter in the points, however, and they do not cluster around the 45° line. Note, however, that the Maritime aerosol model was used for all the calculated extinctions, irrespective of the conditions for that particular block. The subsequent analysis will try to separate the molecular and aerosol contributions to the extinction, and test the appropriateness of different aerosol models under different conditions.

4.2 Separation of Molecular and Aerosol Extinction

The EMI filters were chosen in window regions of the atmosphere, where the molecular absorption is relatively small, and extinction by aerosols becomes significant. The relative importance of the molecular to the aerosol extinction over a range of conditions is shown in Table 1, for each filter. Here, the filter-weighted molecular and aerosol extinction coefficients were calculated separately by LOWTRAN for three visual ranges and three water amounts which cover the

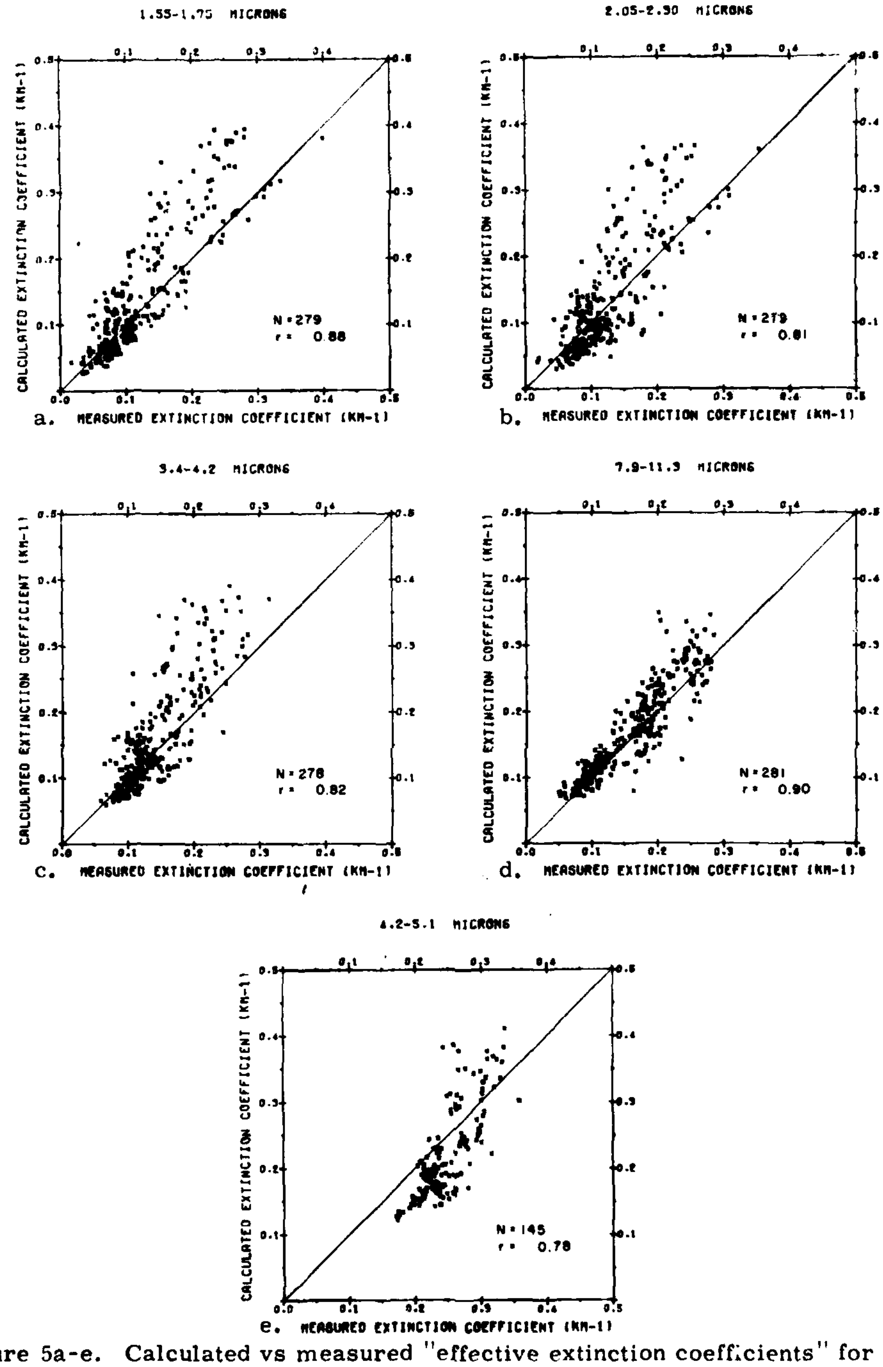

Figure 5a-e. Calculated vs measured "effective extinction coefficients" for filters 2 to 6 for all the 281 usable cases in the EMI data set, using the Maritime aerosol model: a. filter 2, b. filter 3, c. filter 4, d. filter 5, e. filter 6. N is the number of points and r is the correlation coefficient.

Table 1. The ratio of the molecular to the aerosol "effective extinction" coefficients" for three meteorological ranges and three water amounts, spanning the conditions found in the EMI data set. The conditions are: P = 1013 mb, RH = 80 percent, T = 0.3, 10.3, 21.1° C for 5, 10, 20 mb water vapor, Range = 20 km, Maritime aerosol model.

Filter	Absolute Humidity (mb)	Meteorological Range (km) 10	30	90
	5	.03	.08	.31
1. (.57-.97μ)	10	.03	.09	.35
	20	.03	.10	.39
	5	.03	.09	.32
2. (1.55-1.75μ)	10	.03	.10	.38
	20	.04	.12	.45
	5	.04	.14	.53
3. (2.05-2.3μ)	10	.05	.17	.65
	20	.07	.22	.82
	5	.19	.60	2.3
4. (3.5-4.2μ)	10	.23	.76	2.8
	20	.31	1.0	3.7
	5	.67	2.1	7.9
5. (7.9-11.3μ)	10	1.2	3.9	14.4
	20	2.7	8.3	31.2
	5	.47	1.5	5.7
6. (4.2-5.1μ)	10	.53	1.7	6.3
	20	.59	1.9	7.2

range encountered by the EMI data set; the water amounts are 5, 10, and 20 mb and the visual ranges are 10, 30, and 90 km. The pressure is 1013 mb, the relative humidity is constant at 80 percent, and the temperature is the value consistent with the relative humidity and water amount (0.3, 10.3, and 21.1° C for the water amounts 5, 10, and 20 mb). The Maritime aerosol model is used throughout. The conditions prevailing during the measurement series are indicated by Figure 6 which shows a histogram of the number of occurrences vs meteorological range (as calculated in Eq. (9)) and by Figure 7 which shows the histogram for absolute humidity.

From Table 1 and Figures 6 and 7, it is clear that the aerosol extinction strongly dominates the molecular absorption for filters 1, 2, and 3 for almost all cases in the data set. For the 7.9 to 11.3 μ filter, molecular absorption predominates; for the other two filters the situation is mixed.

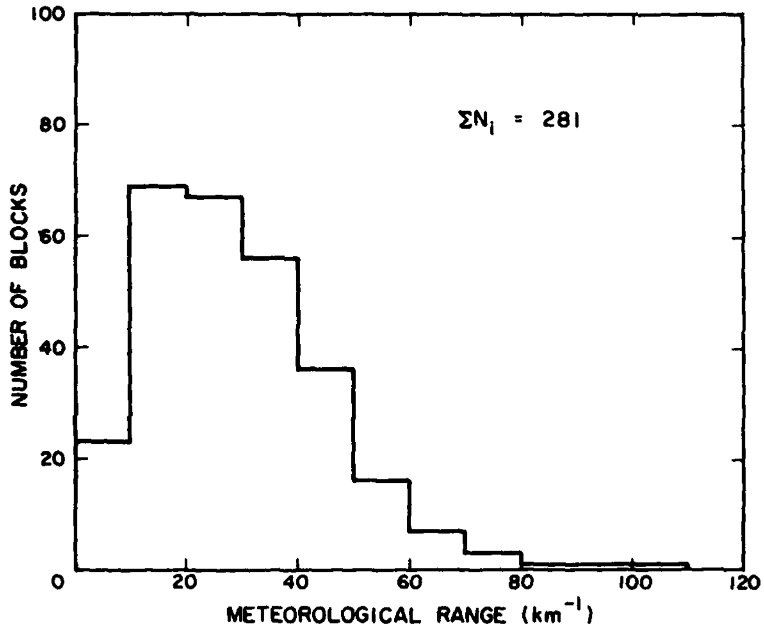

Figure 6. Meteorological range (from Eq. 9) vs frequency of occurrence

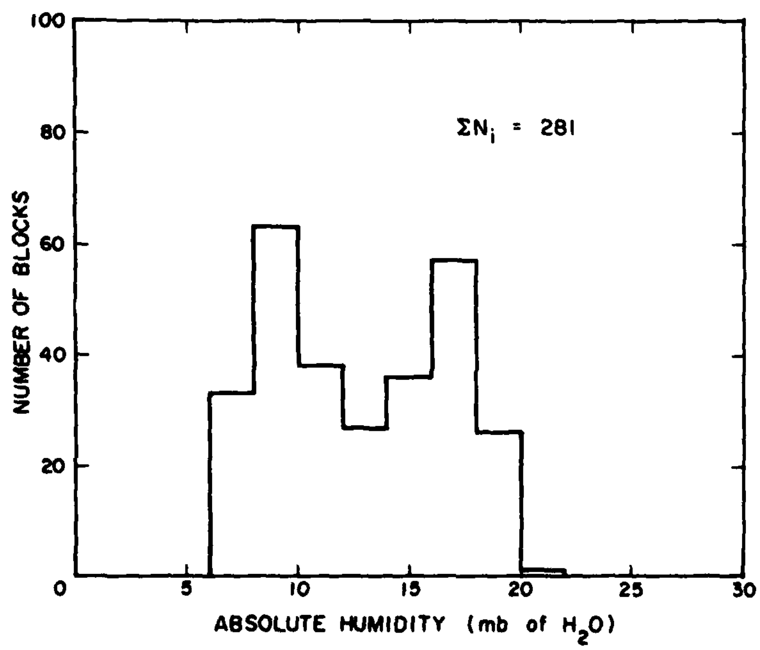

Figure 7. Absolute humidity vs frequency of occurrence

The comparison of the EMI data, therefore, with the LOWTRAN calculations for filters 2 and 3 is essentially a comparison of the measured data with the aerosol part of LOWTRAN. Similarly, the comparison for filter 5 tests primarily the fit of the molecular portion of LOWTRAN with the measurements, especially when only high-visibility cases are considered.

Before considering cases involving aerosol extinction, it is useful to consider the cases dominated by molecular absorption. This comparison will give an indication of both the systematic and the random errors in the measured extinction coefficients.

4.3 Molecular Absorption

Figure 8a shows the measured vs the calculated extinction coefficients for filter 5, for the 50 cases of highest meteorological range. The meteorological ranges vary from 102 km to 43 km, while the water vapor amounts are typically 10 mb; therefore, from Table 1, the mean molecular extinction coefficients are typically 10 times that of the aerosol. The quality of fit is indicated by the correlation coefficient r of 0.94; the slope b of the line is 1.09, the y intercept y_o is -0.002 km^{-1}, and the standard deviation about the regression line is 0.016 km^{-1}.

The accuracy of the calibration of the measurements can be checked using the y intercept of the regression line; if there is no calibration error, the line should pass through the origin. The y intercept of the line is -0.002 km^{-1} which is not statistically different from zero, when compared to the noise in the data. This result, then, indicates that the calibration error is negligible. For this reason, all future plots will be drawn with the regression line constrained to pass through the origin.

Figure 8b shows the same points as Figure 8a but with the y intercept set equal to zero. The slope of the line is now 1.07, indicating that the calculated extinction may be too high by about 7 percent. This discrepancy is surprising in view of the fact that the calculated extinctions from LOWTRAN are based partly on these very same measurements. To explain further, the current water vapor continuum model in LOWTRAN is based on the work of Roberts, et al.[6] In this paper, the water vapor absorption coefficients in the 10 μ region were revised to fit both a subset of the EMI data and a set of laboratory measurements by Burch.[7] The EMI subset consisted of the 103 measurements for the 7.9 to 11.3 μ filter for

6. Roberts, Robert E., Selby, John E., and Bieberman, L. (1976) Applied Optics, 15, 2085.

7. Burch, Darrel E., Gryvnak, David A., and Pembrook, John D. (1971) Investigation of the Absorption of Infrared Radiation by Atmospheric Gases: Water, Nitrogen, Nitrous Oxide, AFCRL-71-0124.

which the observer-estimated visibility was greater than 38 km; this subset contains all of the points shown in Figure 8. Under the conditions applying to the set of measurements shown in Figure 8, the absorption due to the water vapor continuum is from 1 to 2 times that due to water vapor line absorption. Therefore, since the LOWTRAN continuum absorption coefficients are based in part on the measurements shown in Figure 8, the deviation of the slope of the regression line in Figure 8 from 1 requires some explanation.

This discrepancy is resolved by the fact that the analysis by Roberts, et al,[6] of the EMI data assumed that the aerosol extinction was zero. As mentioned before, however, the aerosol extinction under these conditions is about 10 percent of the molecular. Therefore, neglecting the aerosol extinction would tend to an overestimate of the continuum absorption coefficients.

To check this explanation, the calculated extinction coefficients shown in Figure 8b were redone, this time with no aerosol extinction included. The results of this calculation are shown in Figure 8c where the correlation coefficient is 0.93, the slope of the regression line is 0.97, and the standard deviation about the line is 0.016. Clearly, the fit of the calculations to the measurements is better; the deviation of the slope from 1.0 has been reduced from 0.07 to 0.03. If aerosols are ignored, therefore, the calculated extinctions are more consistent with the measured values, as they should be.

One might be tempted to conclude on the basis of Figure 8b that the molecular extinction coefficients and, in particular, its continuum coefficients, in LOWTRAN for the 10 μ window are too high and should be revised again. This suggestion should be treated cautiously for the following reasons: (1) the discrepancy in the slope of the regression line in Figure 8b of 7 percent is not large and may be due to statistical variability; (2) the continuum coefficients in LOWTRAN are based only in part on this data; (3) the discrepancy shown in Figure 8b depends upon the particular aerosol model chosen, which may not be appropriate. For a different aerosol model, the discrepancy might be much less. Therefore, any further revision of the LOWTRAN continuum coefficients should be based on further measurements, preferably ones in which the aerosol extinction is really negligible or, at least, known with better precision.

Returning again to the question of calibration, it is interesting to compare the value of σ_0 used by EMI in their calibration with the equivalent value computed by LOWTRAN. Recall that σ_0 was the "effective extinction coefficient" for filter 5 of case 257: this case had the highest recorded transmittance for filter 5, and the calculated value of σ_0 based on the old data is 0.05 km^{-1}. Using LOWTRAN, the calculated value of σ_0 is 0.08 km^{-1}, for a difference of 0.03 km^{-1}. This difference is much larger than the calibration error indicated previously, but is less

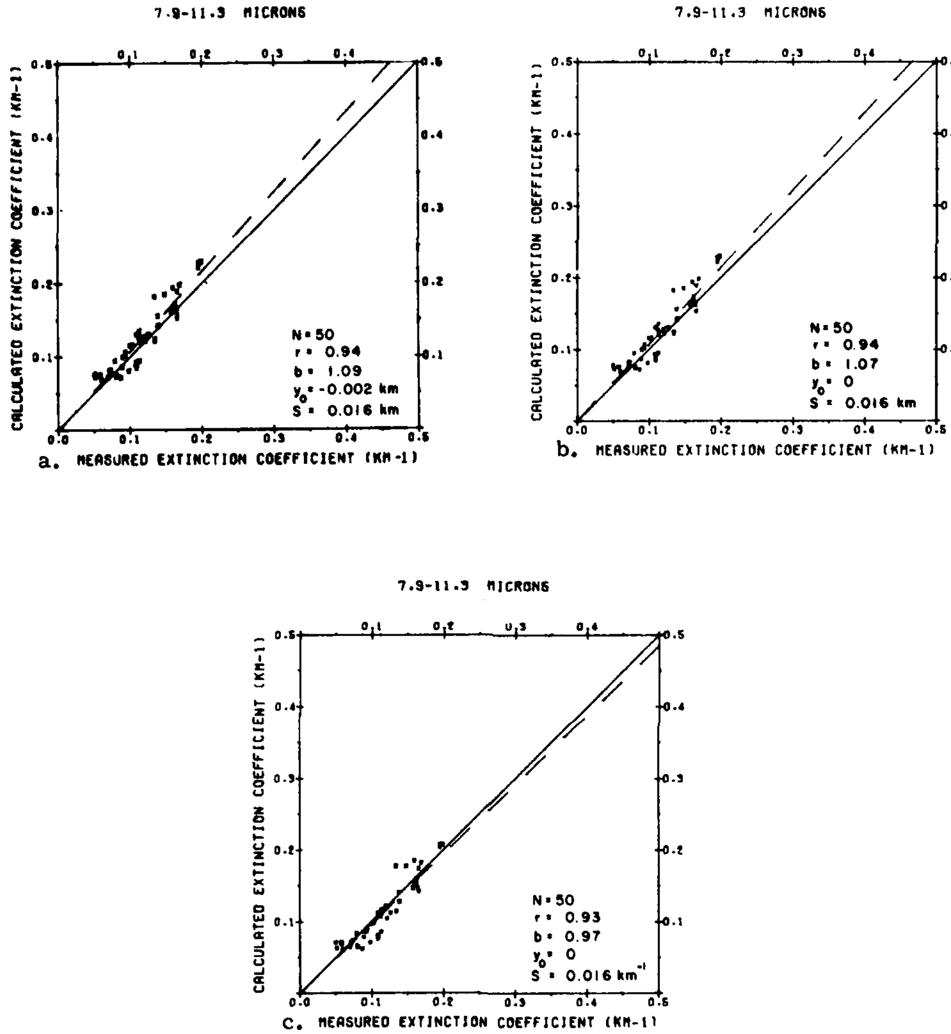

Figure 8. Calculated vs measured "effective extinction coefficients" for filter 5 (7.9 to 11.3 μ) for the 50 cases of greatest meteorological range (from Eq. 9): the solid line is at 45°; the dashed line is a simple linear regression of the calculated data on the measured data. N = number of points, r = correlation coefficient, b = slope, y_o = y intercept, s = standard deviation about the regression line.

a. intercept parameter included in the regression

b. regression through the origin

c. same as b. except with no aerosol extinction in the calculated data

than two standard deviations as shown in Figure 8b. The reason for this difference is not clear, but it appears to be due to random error occurring in both the measured transmittance and in the measured inputs to LOWTRAN, and it is fortuitous that these errors just cancel.

Finally, Figure 8b can also be used to estimate the random error in the data. While simple least squares theory is not strictly valid in this situation, the scatter of points about the regression line is an indication of the combined random error in the measured and the calculated coefficients. The standard deviation about the regression line is 0.016 km^{-1}, so that a good estimate of the combined random error is about twice this, or ± 0.03 km. In transmission, this error translates to a relative error in transmittance of about ± 50 percent. This number gives an upper limit on the random measurement error for filter 5, and it seems likely that the random measurement errors for the other filters are of similar magnitude. Similarly, this number also gives an upper limit on the random errors in the calculated molecular extinction coefficients. This data gives no indication, however, of the errors in the calculated aerosol extinction coefficients alone.

Filter 6 (4.1 to 5.1 μ) is also dominated by molecular absorption, but to a lesser extent than filter 5. Figure 9 shows the comparison of the calculated vs the measured extinctions for the same set of data blocks as in Figure 8: however, since this filter was only used in the summer run, there are only 21 points. Under the conditions applying to these measurements, the molecular extinction is typically five times that of the aerosol. The correlation shown in this figure is good (0.94) but the slope is only 0.73. (If the regression is done including the y intercept as a parameter, the y intercept is found to be 0.002 km^{-1}, again indicating no significant calibration error.) This figure, therefore, indicates a high degree of precision in the measurements, accompanied by a significant systematic error, with the calculated extinction being too low by about 27 percent.

A similar discrepancy between LOWTRAN calculations and measurements was shown by Haught and Cordray.[8] They made measurements of infrared transmittances using a high-resolution FTS system over a 5.1 km path, under conditions of high visibility, and with different amounts of water vapor in the path. Comparison between their measurements between 4.4 and 5.0 μ, degraded to LOWTRAN resolution and LOWTRAN calculations, shows that LOWTRAN systematically predicts too much transmission. Figure 10 shows the results for one particular measurement, taken from their report. The solid line is the measurement and the dotted line is the LOWTRAN calculations. The conditions are 17.3 torr of water vapor at one atmosphere; the temperature is not given but assuming a relative humidity of 80 percent implies an ambient temperature of 23° C. In this particular case,

---

8. Haught, Kenneth and Cordray, D. (1978) Applied Optics, 17, 2668.

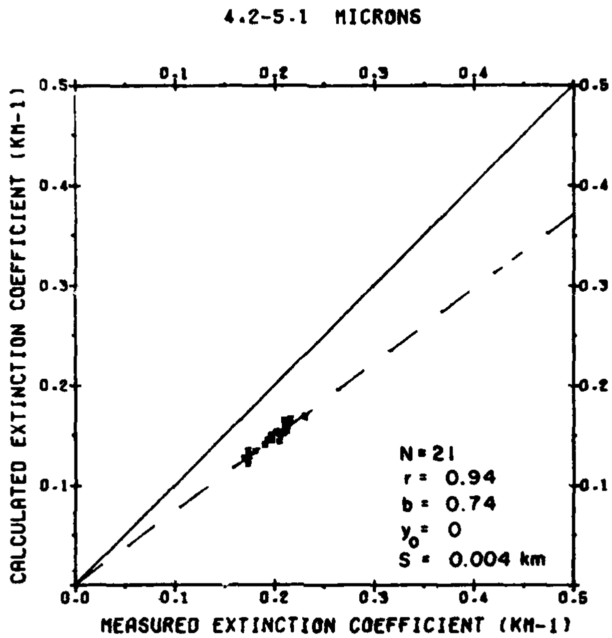

Figure 9. Same as 8b. except for filter 6 (4.2 to 5.1 μ)

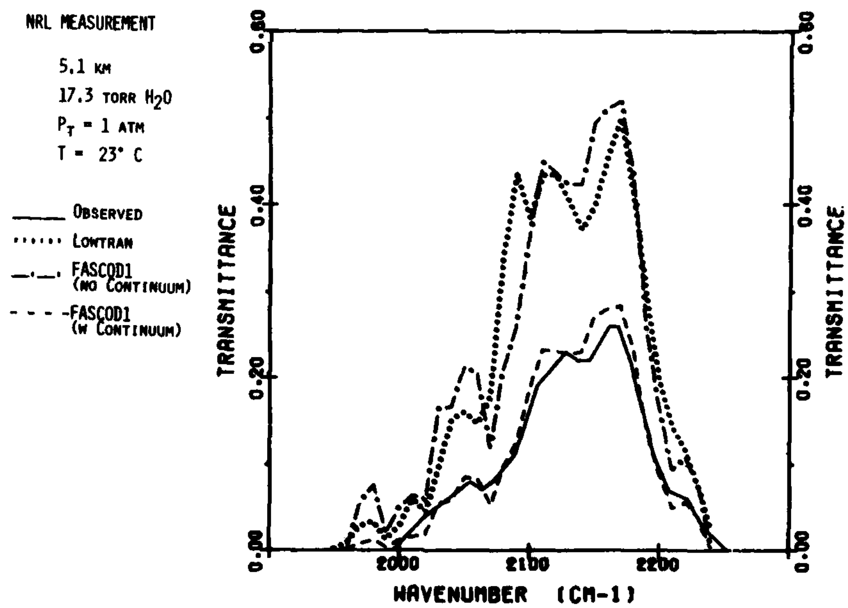

Figure 10. Comparison between NRL measurement (solid line), LOWTRAN calculation (dotted line), and FASCOD1 calculation without a continuum (dashed-dot line) and with a water vapor continuum (dashed line): Range = 5.1 km, P = 1 atm, P_{H2O} = 17.3 torr, RH assumed here to be 80 percent giving T = 23° C

LOWTRAN underpredicts the minimum absorption at 2180 cm^{-1} by 30 percent of the measured absorption. Comparison between the measurements and calculations for other cases shows that the discrepancy is dependent on the water vapor amount; for example, with only 2.5 torr of water vapor in the path, LOWTRAN underpredicts the minimum absorption by only 10 percent relative to the measured absorption.

The fact that the relative discrepancy between the measured and the calculated absorption increases with increasing water-vapor pressure suggests that the discrepancy may be due to a continuum-type absorption; LOWTRAN presently has no continuum in this region. To clarify this point, a calculation was made using the line-by-line program FASCOD1[9] for the same atmospheric conditions both with and without a water vapor continuum; these results are also shown in Figure 10. The results for the line-by-line calculation with no continuum (dashed-dot line) shows a reasonably good agreement with the LOWTRAN calculations, indicating that LOWTRAN is modeling the molecular line absorption correctly. When the FASCOD1 continuum is included (dashed line), the calculated absorption agrees to better than 3 percent of the measured. These results indicate that the discrepancy between the LOWTRAN calculations and measurements is due to the lack of a water vapor continuum in LOWTRAN.

The water vapor continuum used in FASCOD1 merits some discussion here. It is assumed that the continuum absorption is due entirely to absorption by the wings of distant lines (specifically, the wings of lines more than 256 halfwidths away), and that the water-vapor line shape is sub-Lorentzian. The line shape has been adjusted until the calculated continuum at 4 and 10 μ fits the laboratory measurements of Burch.[7]

The present FASCOD1 continuum is only tentative and is being reanalyzed. Work is also underway to see if the FASCOD1 continuum, which spans the entire infrared spectrum, is suitable as a replacement for the LOWTRAN continuum functions which cover only the 3.3 to 4.2 μ and 8 to 14 μ regions. If it is not, a separate empirical continuum will be developed to cover the 4.5 to 5.0 μ region separately and correct the existing deficiency.

---

9. Smith, H. J. P., Dube, D. J., Gardner, M. E., Clough, S. A., Kneizys, F. X., and Rothman, L. S. FASCODE - Fast Atmospheric Signature Code (Spectral Transmittance and Radiance) AFGL-TR-78-0081. Also, Clough S. A. Private Communication.

4.4 Validation of the Aerosol Models

The calculated extinction coefficients shown in Figure 5 were all computed using the Maritime aerosol model. This model was developed for open-sea conditions with moderate windspeed. The measurements were made on the coast, however, where the wind was sometimes offshore and was of variable intensity; it is not likely that a single aerosol model would fit all of these cases. Indeed, a close look at Figures 5b and c shows that the points for σ greater than about $0.1\ km^{-1}$ fall naturally into two distinct groups: one group clusters around the 45° line while the other group lies well above it. A detailed analysis shows that the points around the solid line correspond to mostly moderate onshore winds, while those above the line are mostly offshore winds or light breezes.

To test this relationship, the cases shown in Figure 5 were grouped into the onshore cases ($170° \le \theta \le 250°$, where θ is the wind direction) and the offshore cases ($\theta \le 100°$ and $\theta > 320°$). The wind directions delimiting these two groups are somewhat arbitrary but the results depend very little on the precise boundaries. Figure 11 shows a histogram of wind direction vs frequency of occurrence. Winds

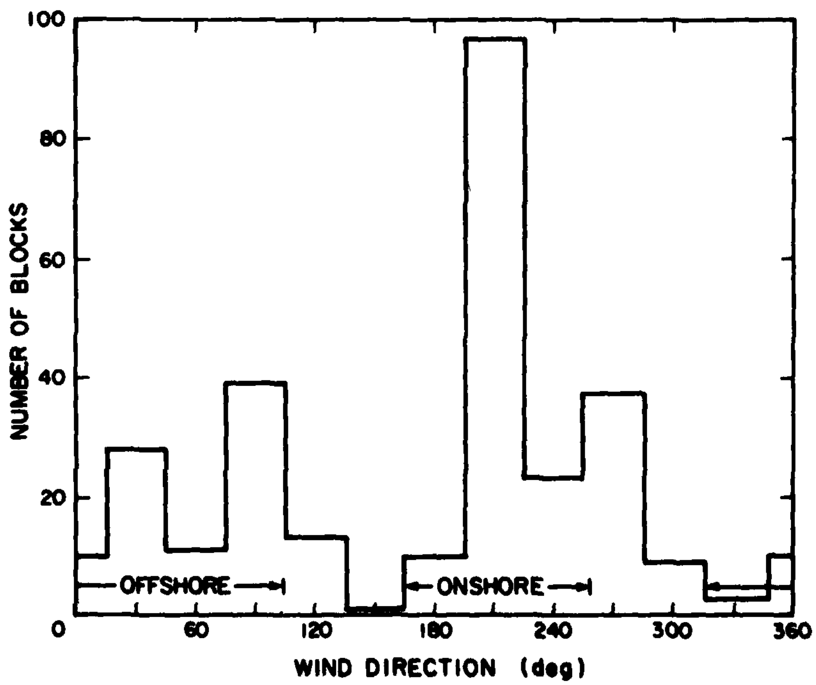

Figure 11. Wind direction vs frequency of occurrence

from 110° to 160° and from 260° to 310° seem to be of mixed origin and are not included in this sample; but, from Figure 11, these cases represent only one quarter of the total cases. The onshore winds were divided further into light winds -- those of wind speeds less than 5.5 m sec^{-1} (3 or less on the Beaufort scale) -- and moderate winds -- those with wind speeds between 5.5 m sec^{-1} and 17 m sec^{-1} (4 to 7 on the Beaufort scale). These three groups are plotted individually in Figure 12 (moderate onshore winds), Figure 13 (offshore winds), and Figure 14 (light onshore winds). The number of cases of strong onshore winds is too small for reliable statistics so these points are not shown.

Consider Figure 12a, the plot for filter 2 for the cases of moderate onshore winds. Here the fit of the calculated to the measured points is good; the slope of the regression line is 0.95, and the standard deviation of the points about this line is 0.013 km^{-1}. The fits for filters 3 and 4 shown in Figures 12b and c are almost as good; however, the standard deviations in these filters are almost twice that for filter 2.

The corresponding plots for these filters for the offshore wind cases shown in Figures 13a, b, and c show that the calculated extinction is much too large, by almost a factor of 2 for the high extinction cases. The scatter of points about the regression line is also larger than in Figure 12 by a factor of 2.

The plots for the cases of light onshore winds shown in Figures 14a, b, and c fall somewhere between those for the moderate onshore winds and the offshore winds; most of the points are clustered down in the region of low extinction, while the few points of high extinction are scattered.

Now consider the plots for filter 5 for the three categories, shown in Figures 12d, 13d, and 14d. The best fit is, as expected, in Figure 12d, for the cases of moderate onshore winds. Here the slope of the regression line is not significantly different from 1, while the standard deviation of 0.017 km is the same as in Figure 8b. (Note, however, that some of the points in Figure 8b and 12d are the same.) The fit for the offshore cases shown in Figure 13d, however, is not much worse; the slope of the regression line is only slightly larger than in Figure 12d (and is about the same as in Figure 8b) while the standard deviation is only twice as large. The plot for the light onshore winds shown in Figure 14d is about the same as in Figure 13d; the slope is slightly larger and the scatter slightly less.

The plots for filter 6, shown in Figures 12e, 13e, and 14e are a bit more difficult to interpret but generally support the same conclusions as the plots for the other filters. The plot for the moderate onshore winds, Figure 12e, has the same slope as in Figure 9; it reflects the lack of water-vapor continuum in the calculated transmittances but is also compatible with the good fit of the Maritime model to the data seen in Figures 12a, b, and c. The offshore-wind cases in Figure 13e again indicate that the Maritime model predicts too much absorption, while the light onshore wind cases in Figure 14e again show mixed results.

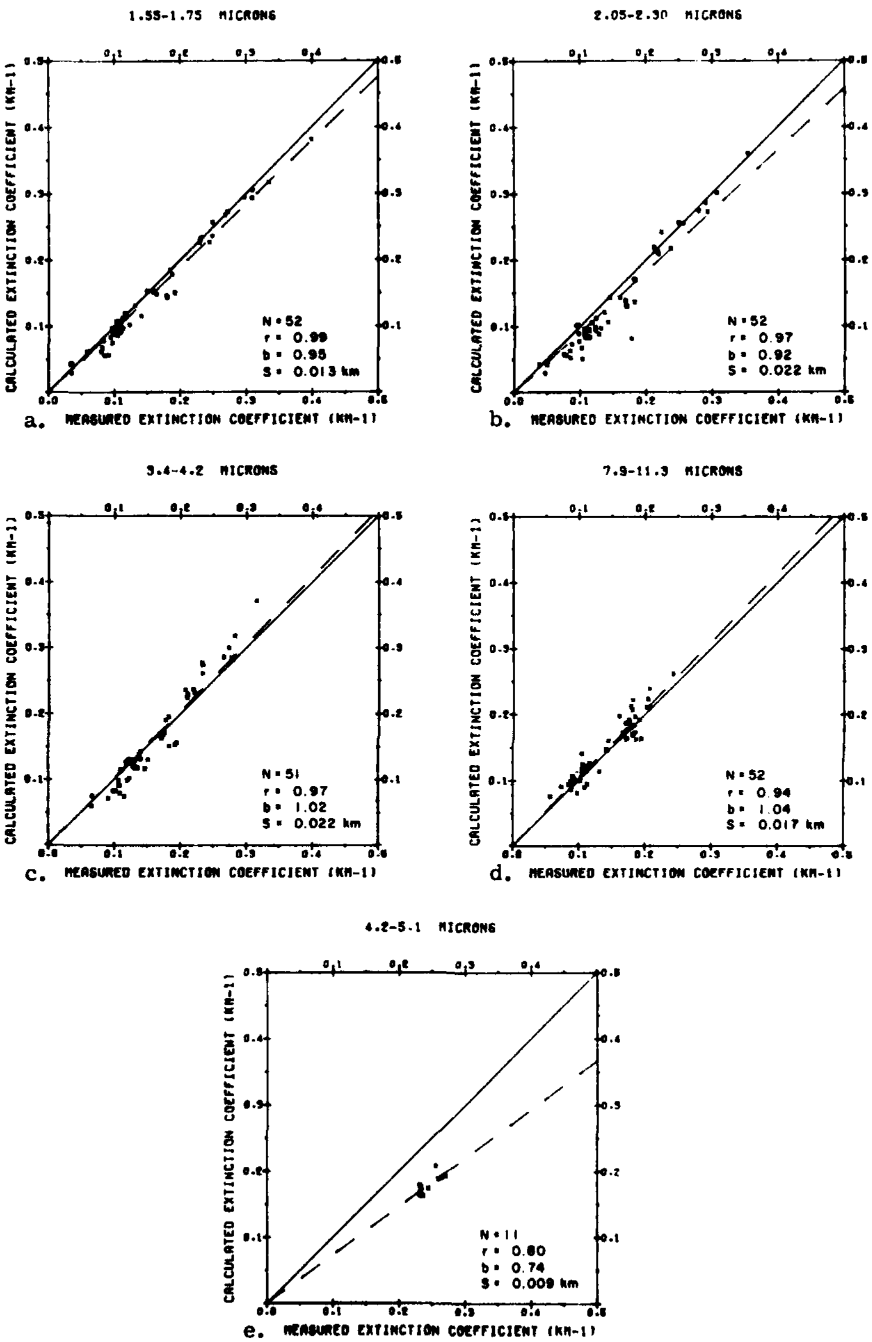

Figure 12. Calculated vs measured "effective extinction coefficients" for the cases of moderate, onshore winds, Maritime aerosol model

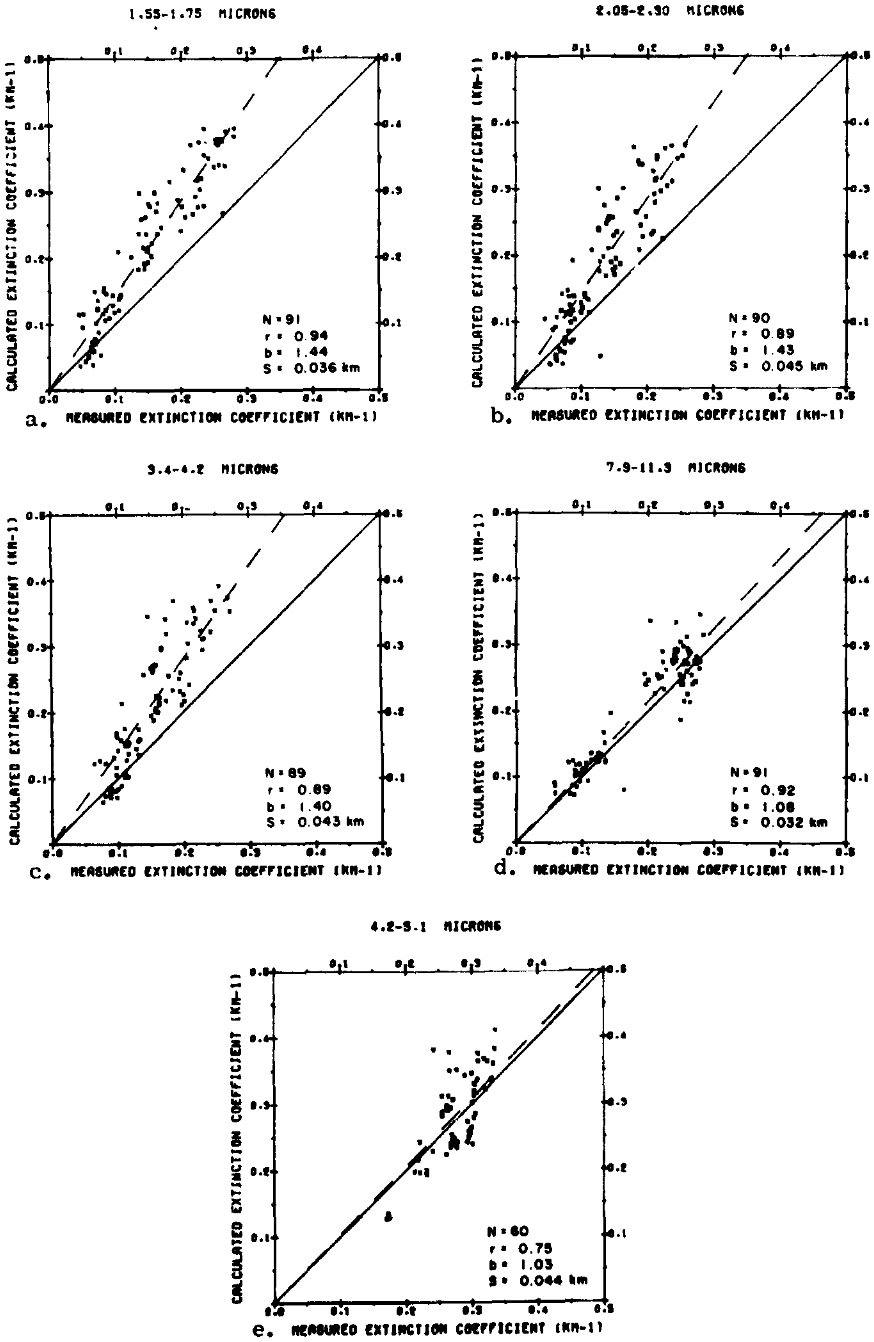

Figure 13. Calculated vs measured "effective extinction coefficients" for the cases of offshore winds, Maritime aerosol model

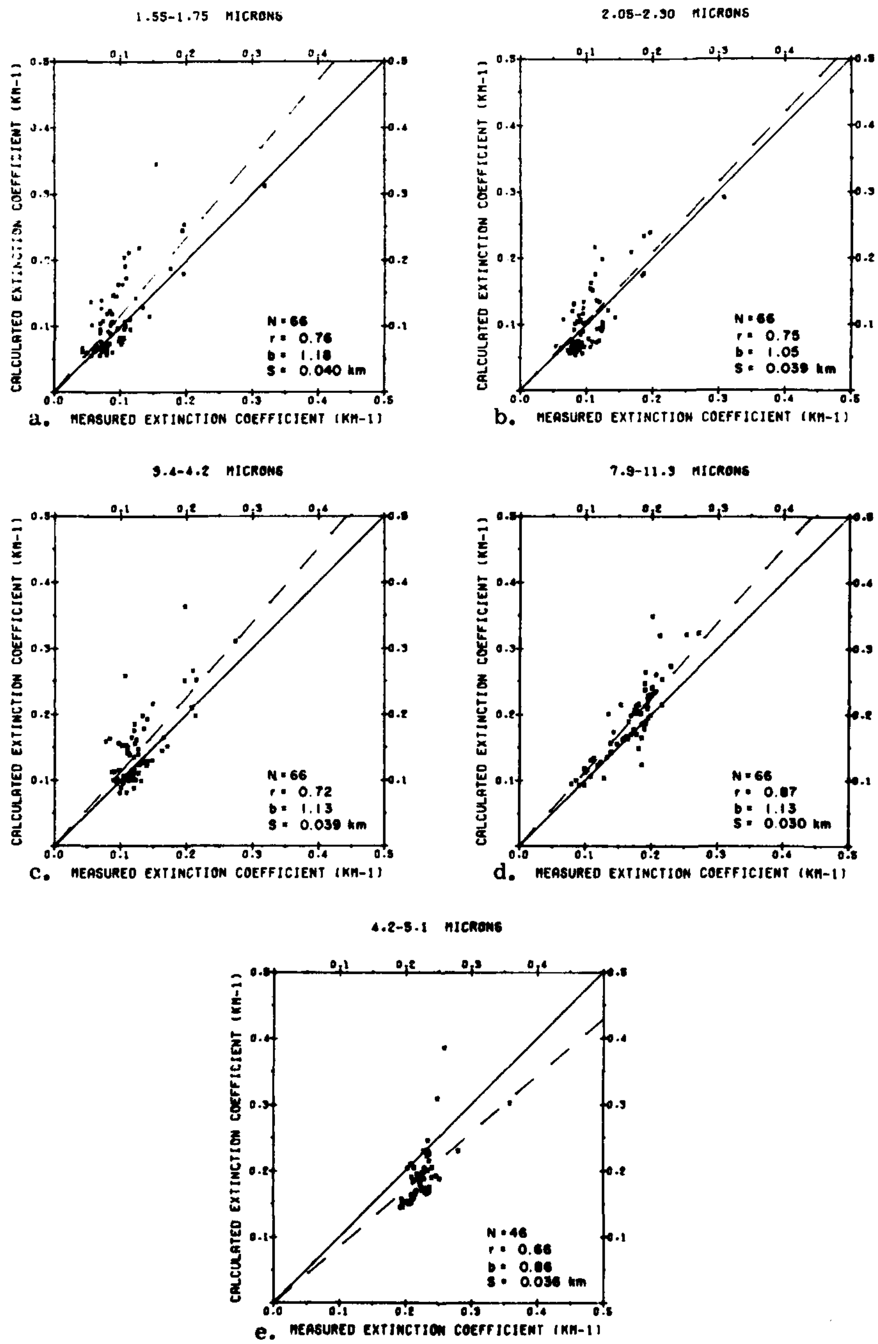

Figure 14. Calculated vs measured "effective extinction coefficients" for the cases of light onshore winds, Maritime aerosol model

These results are readily explained in terms of the aerosol model. The Maritime aerosol model contains a relatively large number of large particles of oceanic origin which are raised by the wind. From Figure 3, it is seen that the inclusion of these large particles in the Maritime model decreases the fall-off of the extinction coefficient with wavelength, compared to the Rural model. Clearly, the cases of moderate offshore winds shown in Figure 12 are described well by the Maritime model. Offshore winds, however, carry few of these large particles, so that the Maritime model predicts too much extinction (Figure 13). The cases of light onshore winds (Figure 14) fall somewhere in between these two extremes.

The increased scatter in the offshore and light onshore cases, compared to the moderate onshore cases, can be interpreted as indicating that the aerosol composition for the moderate onshore cases is more uniform than that for the offshore or light onshore cases.

Since the Maritime model overpredicts the aerosol extinction for the offshore cases, these cases were recalculated using the Rural model and are shown in Figure 15. The value of 0.659 was used for β in Eq. (9) to adjust the slope of the regression line for filter 1 (not shown) to approximately 1. Figures 15a-e show that the Rural model underpredicts the aerosol extinction in these cases by about as much as the Maritime model overpredicts it. The explanation for this result is that although the wind comes off the land, the optical path is over water and several kilometers from shore. Therefore, some large oceanic particles are probably present which are not accounted for in the Rural model. From Figures 13 and 15, the appropriate model for these offshore winds is approximately an average of the Rural and the Maritime models.

Comparison of the plots for filter 5, for the different cases and aerosol models, also demonstrates again the fact that the aerosol extinction in 10 μ region is less important relative to the total extinction than in the 3 to 5 μ region. When making calculations in the 10 μ region, therefore, the choice of the aerosol model and the value used for the meteorological range are less critical than in the 3 to 5 μ region.

4.5 Relative Humidity Dependence

The calculated aerosol extinction coefficient is a function of both the meteorological range and, to a lesser extent, the relative humidity. The effect at work here is that, as the relative humidity increases, aerosol particles tend to accrete liquid water, resulting in changes in the particle size distribution and in the mean refractive index. Figure 16 shows the relative humidity dependence of the calculated aerosol extinction coefficient for the Maritime model. The question has been raised whether the inclusion of the relative humidity dependence in the aerosol-extinction coefficient results in an improved fit between LOWTRAN calculation and measurements.

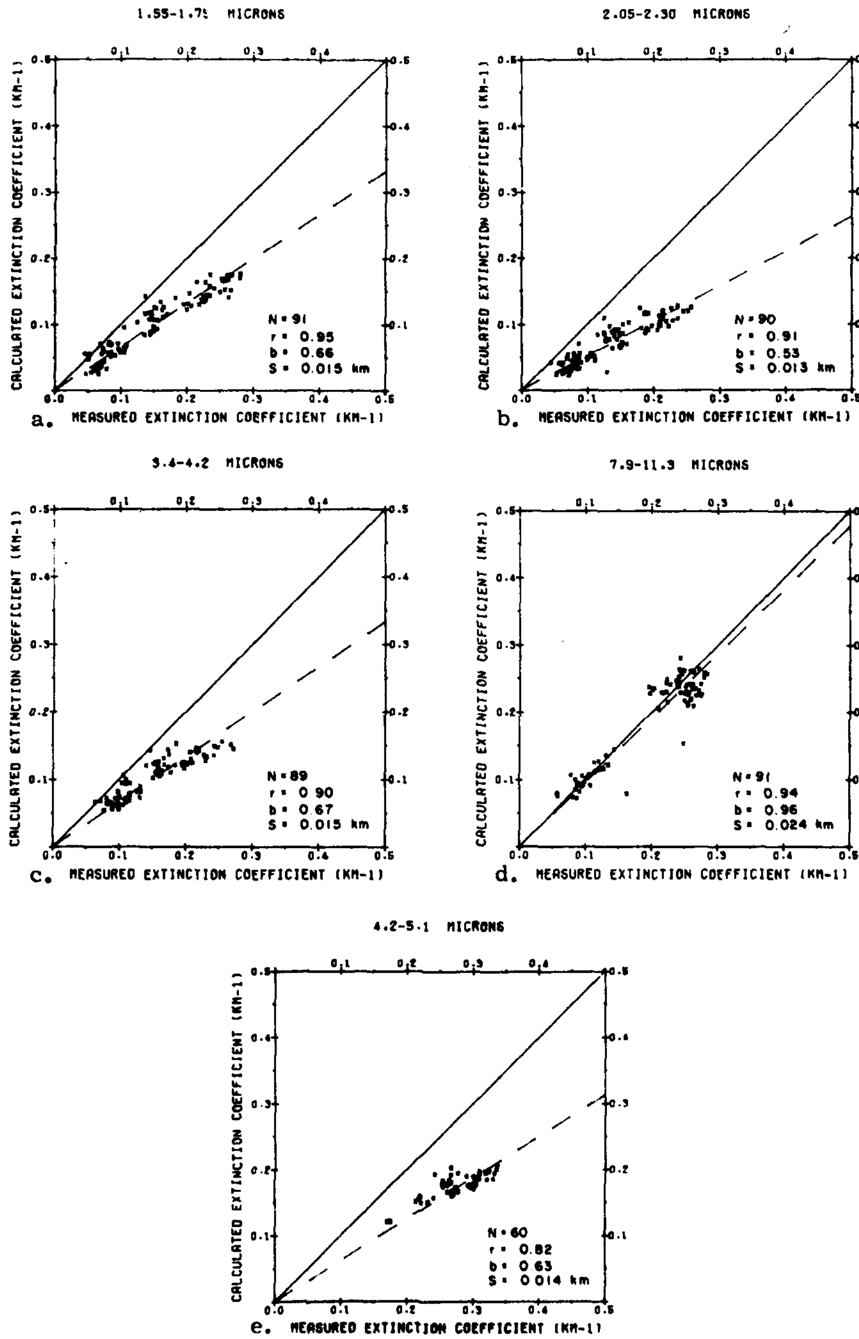

Figure 15. Calculated vs measured "effective extinction coefficients" for the cases of offshore winds, Rural aerosol model

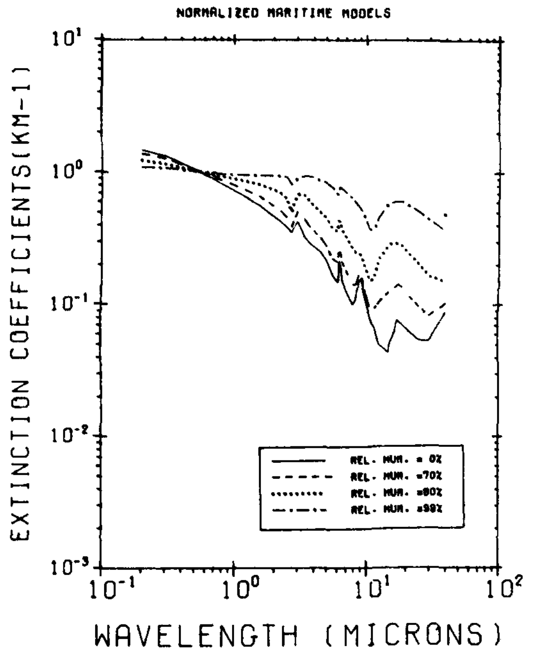

Figure 16. Relative humidity dependence of the Maritime aerosol model extinction coefficient

To answer this question, the cases shown in Figure 12 (onshore winds of moderate intensity) were recalculated using a fixed (arbitrary) value of 90 percent in the calculation of the aerosol-extinction coefficient. The correct water vapor amount was used in the calculation of the molecular extinction. The results of this calculation are shown in Figures 17a-e. A comparison of these plots with Figures 12a-e shows that neglecting the relative humidity dependence of the aerosol extinction actually leads to a small improvement in the fit between the measured and calculated data. While changes in the slope of the regression lines are insignificant, the standard deviations around the lines have decreased, by as much as a factor of two for the 3.4 to 4.2 μ filter.

This result is both surprising and disturbing. It is well known that the particle size distribution changes with relative humidity, yet this data shows that a fixed relative humidity model fits better than a variable one. Before accepting the conclusion, however, that the relative-humidity-dependent aerosol model is deficient, the conditions of the measurements must be examined more carefully.

The relative humidity was measured by a wet and dry bulb thermometer in an enclosure on the beach at one end of the path. It, therefore, measures only the local value of the relative humidity. The optical path, however, is mostly over water, with the point of closest approach between the beam center and the sea varying between 1 and 7 m. The mean relative humidity along the path, however,

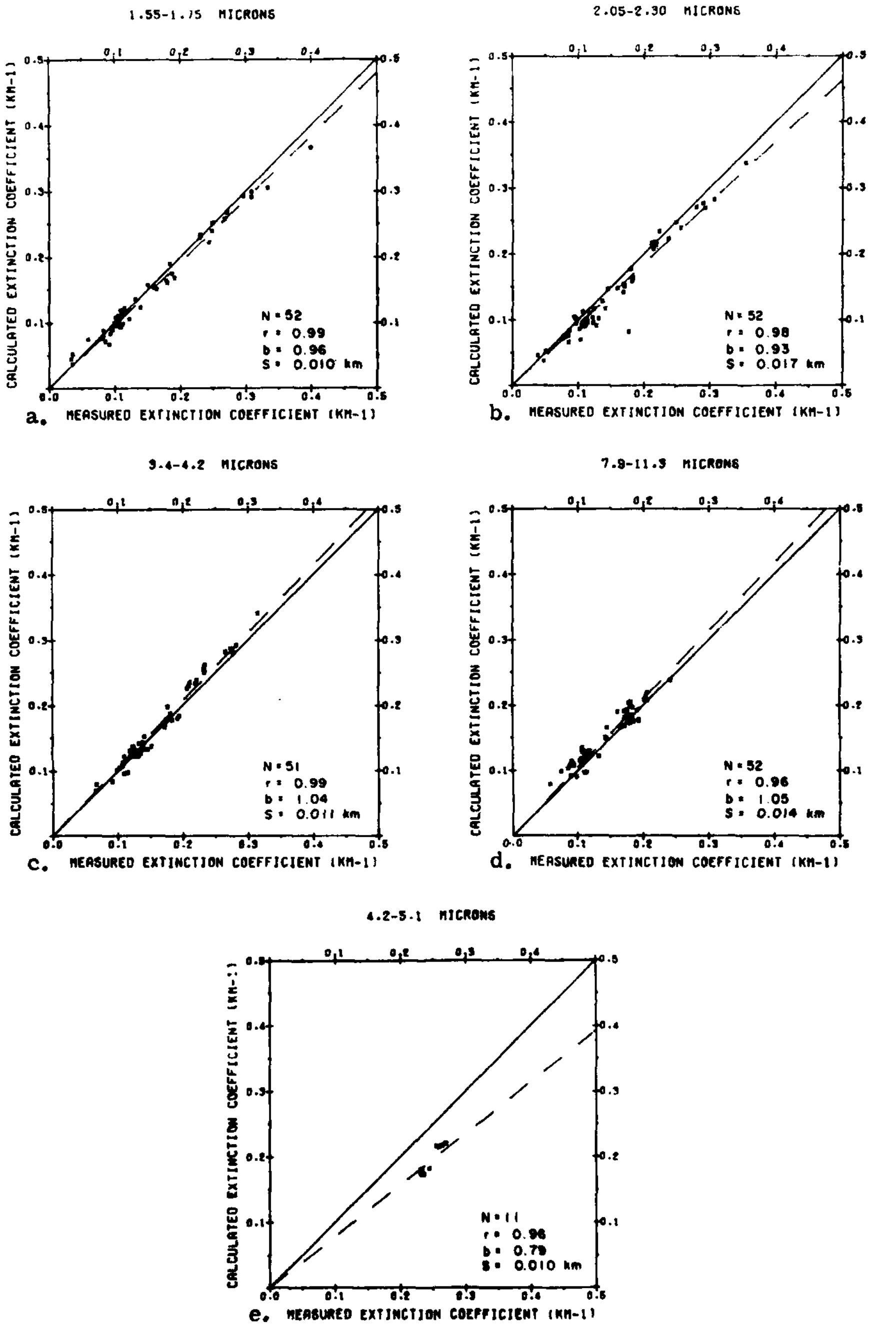

Figure 17. Calculated vs measured "effective extinction coefficients" for the cases of moderate onshore winds, using the Maritime aerosol extinction coefficient for 90 percent relative humidity

may quite possibly be significantly different from the measured value; specifically, the value over the water is likely to be consistently higher, and perhaps less variable, than the measured value on the beach.

Figure 15 shows that extinction coefficient for the Maritime model is very sensitive to the relative humidity. For example, an error of 5 percent in the relative humidity for a relative humidity of 80 percent at 3.75 μ produces a 15 percent error in the extinction coefficient.

The measured value of the relative humidity, therefore, may not reflect the actual value along the path, and it may be this discrepancy which explains the poor performance of the relative-humidity-dependent model compared to the fixed-relative-humidity model. A more reliable verification of the relative-humidity-dependent model would require measurements along a more completely instrumented path; for example, with measurements of relative humidity made at several points along the path.

5. SUMMARY AND CONCLUSIONS

This report has presented the results of a comparison of broadband infrared transmittances measured over a 20 km path over water with transmittances calculated by LOWTRAN. The goal has been to validate the Maritime aerosol model in LOWTRAN and to test the calculated molecular extinction in the 4.5 to 5.0 and 8 to 12 μ window regions.

The results have shown that the calibration of the measurements is good; that is, the calibration error is negligible compared to the noise in the data. An upper limit on the random error in the measurements, including the combined effects of errors in the transmittances, temperature, and relative humidity, is estimated to be $\pm$ 0.03 km^{-1} in the "effective extinction coefficient" or about a $\pm$ 50 percent relative error in the transmittance.

For the cases of high visibility, the aerosol extinction in the 8 to 12 μ and the 4.5 to 5.0 μ window regions is small compared to the molecular extinction, allowing the molecular extinction to be evaluated separately. Analysis of these cases indicates that the LOWTRAN water vapor continuum absorption coefficient in the 8 to 12 μ region may be too large by about 7 percent; however, this point needs to be clarified with more measurements. The results seen here for the 4.2 to 5.1 filter, along with the results in reference 9, also show that LOWTRAN seriously underpredicts the absorption in this region due to a lack of a water-vapor continuum.

Looking at cases for which aerosol extinction is important, the results show that for cases of onshore winds of moderate intensity, the Maritime aerosol model provides a good fit to the measured data. For the cases of offshore winds, the Maritime model predicts too much extinction, while the Rural model predicts too little. Removing the relative humidity dependence from the Maritime aerosol model actually leads to a slight improvement in the fit between the calculations and the measurements. This result, however, may be due more to deficiencies in the measurements than in the model.

References

1. Arnold, D. H., Lake, D. B., and Sanders, R. Comparative Measurements of Infrared Transmission Over a Long Sea Path, E.M.I. Reports DMP 3736 (1970) and DMP 3858 (1971).

2. Altshuler, T. L., Infrared Transmission and Background Radiation by Clear Atmospheres, General Electric Co. Missile and Space Vehicle Department, Valley Forge, PA, Report No. 61SD19 (Dec 1961) (Available from NTIS - Accession Number AD 401923).

3. Hudsen, K. D. (1969) Infrared Systems Engineering, Ch 4, John Wiley and Sons, New York.

4. Kneizys, F. X., Shettle, E. P., Gallery, W. O., Chetwynd, J. H., Jr., Abreu, L. W., Selby, J. E. A., Fenn, R. W., and McClatchey, R. A. (1980) Atmospheric Transmittance/Radiance: Computer Code LOWTRAN 5, AFGL-TR-80-0067.

5. Shettle, E. P. and Fenn, R. W. (1979) Models for the Aerosols of the Lower Atmosphere and the Effects of Humidity Variations on Their Optical Properties, AFGL-TR-79-0214, AD A085951.

6. Roberts, Robert E., Selby, John E., and Bieberman, L. (1976), Applied Optics, 15, 2085.

7. Burch, Darrel E., Gryvnak, David A., and Pembrook, John D. (1971) Investigation of the Absorption of Infrared Radiation by Atmospheric Gases: Water, Nitrogen, Nitrous Oxide, AFCRL-71-0124, AD 88276.

8. Haught, Kenneth and Cordray, D. (1978) Applied Optics, 17, 2668.

9. Smith, H. J. P., Dube, D. J., Gardner, M. E., Clough, S. A., Kneizys, F. X., and Rothman, L. S. (1978) FASCODE - Fast Atmospheric Signature Code (Spectral Transmittance and Radiance) AFGL-TR-78-0081, AD A057506. Also, Clough, S. A. Private Communication.